Effect of Micelle Composition on the Formation of Surfactant-Templated Polymer Films

Benjamin M. D. O'Driscoll, Cristina Fernandez-Martin, Roland D. Wilson, Stephen J. Roser, and Karen J. Edler*

Department of Chemistry, University of Bath, Bath, Avon, UK, BA2 7AY

Received: October 21, 2005; In Final Form: January 6, 2006

Surfactant-templated polymer films prepared from polyethylenimine (PEI), cetyltrimethylammonium bromide (CTAB), and octaethylene glycol monohexadecyl ether ($C_{16}E_8$) were examined and the effect of increasing the percentage of nonionic surfactant in the micelles measured using both surface and bulk-sensitive techniques. It was found that there is a strong interaction between CTAB and $C_{16}E_8$, although no interaction between the $C_{16}E_8$ and PEI was observed. Generally, increasing the percentage of $C_{16}E_8$ in the micelles decreases both the thickness and degree of order in the films; however, it was observed, depending on the conditions, that films could still be formed with as little as 20% cationic surfactant. Experiments on the CTAB/Brij56/PEI system were also performed and these indicate that it is similar to the CTAB/$C_{16}E_8$/PEI system.

Introduction

Polymer−surfactant systems have been the subject of many investigations over recent years. These self-assembling materials are well-known to form precipitates containing ordered liquid crystalline structures that are being investigated for applications in drug delivery, flavor encapsulation, and triggered release systems. Polymer and surfactant adsorption at interfaces is relevant to a number of industrial applications, primarily for use in personal care products. In previous papers[1,2] we reported the formation and properties of spontaneously assembling solid films of cetyltrimethylammonium bromide (CTAB) and polyethylenimine (PEI) at the air/water interface. The films can be several microns thick and consist of an ordered array of rodlike CTAB micelles encased in polymer. While the formation of mixed surfactant and polymer films occurs in a number of systems (see ref 2 for a review of these), the films formed by CTAB and PEI are unique as both the surfactant and polymer carry a positive charge, though this is only a residual charge in the case of the polymer. Consequently, by adjusting the pH of the solution it is possible to alter the charge on the polymer and in doing so tune the properties of the film, such as the thickness and spacing between micelles, to some degree. If the charge on the polymer is greatly increased, then film formation is completely prevented.

In this paper, we report experiments using the nonionic surfactants octaethylene glycol mono-hexadecyl ether ($C_{16}E_8$) and Brij56 (polydisperse $C_{16}E_{10}$) as a second surfactant. By altering the relative percentages of nonionic and ionic surfactants in the solution, we aimed to determine the effect lowering the micellar charge had on the properties of the film. Although there are no studies in the literature on the CTAB/$C_{16}E_8$ mixed systems, there are a number that report the properties of similar systems, such as CTAB with other monodisperse alkyl poly(ethylene glycol) (C_XE_Y) surfactants[3−6] or CTAB with Brij-type surfactants (polydisperse analogous of the C_XE_Y surfactants),[7,8] one of which examines the CTAB/Brij56 system.[9] For the most part these studies analyzed the mixing of the two surfactants using the regular solution theory approach of Rubingh.[10] According to this theory, the critical micelle concentration of the mixed system (CMC_M) is related to the CMC of the two components (1 and 2) by

$$\frac{1}{CMC_M} = \frac{\alpha}{f_1 CMC_1} + \frac{1-\alpha}{f_2 CMC_2} \quad (1)$$

for which the activity coefficients f_1 and f_2 are given by

$$\ln f_1 = \beta(1-\chi)^2 \quad (2)$$

$$\ln f_2 = \beta\chi^2 \quad (3)$$

where

$$\beta = N_A(W_{11} + W_{22} - 2W_{12})/RT \quad (4)$$

and α and χ respectively are the mole fraction of component 1 in the solution and in the micelles, N_A is Avogadro's number, R is the gas constant, and T is the temperature. Unlike the ideal mixing case,[11] Rubingh's theory takes into account the various interactions between the surfactant molecules (W_{11}, W_{22}, and W_{12}) in the micelle, the sum of which is incorporated into the interaction parameter β.

For the five literature systems in which the mixing behavior is analyzed using this theory—CTAB/Brij56,[9] CTAB/$C_{12}E_4$,[3] CTAB/$C_{12}E_8$,[4] CTAB/Brij35 (polydisperse $C_{10}E_{23}$),[7] and CTAB/Brij93 (polydisperse $C_{18}E_{10}$)[8]—negative β values were calculated, indicating that there is a significant attractive interaction between the nonionic and cationic surfactants.

Analysis of the CTAB/$C_{16}E_8$/PEI samples was principally by neutron reflectometry, which measures the structure of the films normal to the air/water interface, and small-angle neutron scattering (SANS), which measures the size of the micelles in the solution. These were accompanied by Brewster angle microscopy (BAM) and surface tension measurements. Some neutron reflectometry experiments were also performed on mixed CTAB/Brij56 films.

Experimental Section

CTAB was purchased from Acros Organics, $C_{16}E_8$ was from Nikkol Chemicals, and PEI (∼2000 Da, as a 50% weight

* Corresponding author. Telephone: +44 1225 384192. E-mail: K.Edler@bath.ac.uk.

10.1021/jp056032w CCC: $33.50 © 2006 American Chemical Society
Published on Web 03/01/2006

solution of ethylenimine-*N*-(2-aminoethyl)ethylenimine copolymer in water) and Brij56 were from Sigma-Aldrich. The deuterated (D33) CTAB used in the SANS experiments was obtained from CDN Isotopes. All the solutions were made up in Milli-Q water (18.2 MΩ cm) and/or D_2O (in the case of the neutron experiments). The composition of the mixed micelle is defined in terms of the mole percentage of CTAB in the solution, except for solutions containing $C_{16}E_8$ only. For the surface tension measurements the total surfactant concentration was varied, while for the BAM, SANS, and neutron reflectometry experiments it was held constant at 0.037 M. The PEI concentration was defined relative to a standard concentration (designated in this paper as concentration 1) equal to 60 g/L or ≈1.39 mol of monomeric unit/L. Therefore, a 1/4 PEI solution has a quarter of this concentration (15 g/L). No PEI was used in the surface tension measurements. In previous experiments it was determined that the amine groups on the polymer were about 3% charged (pH 11) under the above conditions.[2]

Depending on the measurement, different vessels were used to hold the solutions; for the reflectometry and BAM experiments, poly(tetrafluoroethylene) troughs were used; for the surface tension measurements, glass bottles were used; and for the SANS experiments, standard quartz Hellma cells, with a 1 mm path length, were used. All the solutions were measured at approximately 25 °C, which is above the Krafft point of mixed PEI/CTAB solutions (approximately 20 °C), with the container open to the atmosphere to allow for evaporation, except in the case of the SANS experiments.

The neutron reflectometry and SANS data were collected on the SURF and LOQ instruments, respectively, at the ISIS Pulsed Neutron and Muon source, Rutherford Appleton Laboratories, Chilton, England. The incident angle used for the reflectometry experiments was 1.5°, with data being collected between 0.048 and 0.613 $Å^{-1}$ in Q_Z ($=4\pi \sin\theta_Z/\lambda$). The measurement of each reflectometry profile was broken up into several time periods (each 15 min long), to ascertain whether there was any time dependence in the film formation. For all the films equilibrium was reached within 45 min, and the reported reflectometry profiles were collected after this period, unless otherwise stated. No background was subtracted from these profiles. Where possible, the neutron reflectometry profiles were modeled using the Parratt program (Hahn−Meitner Institute).[12] For all the neutron reflectometry measurements D_2O was used as the solvent instead of water, though a small volume of water was always present in the 50% PEI solution obtained from the suppliers. Due to the large volume of the solutions required for reflectometry measurements, the expense of D33-CTAB, and the tendency of the polymer to exchange protons with the solvent, altering its scattering length density to be close to that of the solvent, only one contrast could be usefully measured for these solutions.

For the SANS measurements three different isotope contrasts were used. For the systems without PEI, fully protonated CTAB and $C_{16}E_8$ were dissolved in 100% and 60% D_2O. For the systems with PEI, protonated CTAB and $C_{16}E_8$ with 100% D_2O were again used with the other contrast being D33-CTAB and protonated $C_{16}E_8$ with 40% D_2O as the solvent. The wavelengths collected ranged from 0.09 to 0.285 $Å^{-1}$ in Q, with each sample being measured for 20 min. The data were corrected for background and reduced to one dimension by radial averaging using the Collette program on LOQ and modeled using a procedure written by Dr. Steve Klein at the NIST Centre for Neutron Scattering for the Igor PRO platform (WaveMetrics). This procedure utilizes a least-squares fitting method that models multiple data sets as a uniform ellipsoid for the shape of the micelles in the solution, where the ellipse is defined using two radii, R(a) and R(b). Interactions between micelles were accounted for using the Hayter−Penfold[13] formalism for describing interactions between charged micelles in solution. For all the models the dielectric constant of the solution was approximated to be that of water (80) and the temperature and charge on the micelle set at 298 K and 25, respectively. The two contrasts for a given surfactant composition and polymer concentration were then modeled simultaneously. A principle problem associated with this use of the ellipsoid model is its inability to distinguish between the two elliptical shapes possible, namely, the prolate (rugby ball-shaped) and oblate (discus-shaped) ellipsoids. For each system equally good fits where obtained for the prolate and oblate models, with both models giving approximately equal ellipse volumes [R(a) × R(b) × R(b)]. For the majority of the systems, we examined the prolate ellipsoid model, which yielded results that were more consistent with our earlier results on this system,[2] so the oblate ellipsoid results were discarded.

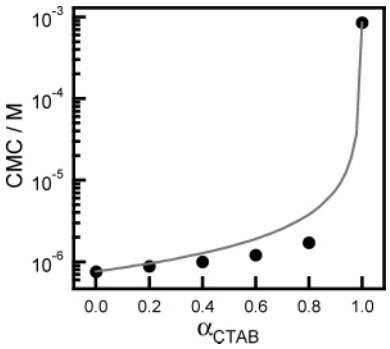

Figure 1. Plot of the CMC of CTAB/$C_{16}E_8$ solutions against the mole fraction of CTAB (α_{CTAB}). The gray curve indicates the expected CMC behavior for ideal mixing ($\beta = 0$).

Surface tension measurements were performed using the breaking surface tension method with paper Wilhelmy plates and a tensiometer from NIMA technologies (Coventry, England). The solutions were prepared in fluoroethylenepropylene bottles, transferred to a glass container, and allowed to equilibrate for 40 min before the surface tension was measured.

BAM images were collected using a NFT Nanoscope2 Brewster angle microscope.

Results and Discussion

Surface Tension. From plots of the surface tension against the concentration, the CMC of a number of different CTAB/$C_{16}E_8$ molar ratios were determined; a plot of these CMC against the CTAB mole fraction (α_{CTAB}) is shown in Figure 1.

Consistent with the literature,[3,4,8,14] the measured values for the CMC of the CTAB/$C_{16}E_8$ mixed films are less than those calculated for the ideal mixing case, so there is an enhanced attractive interaction between the molecules in the micelles. Subsequently, following the methodology of Rubingh,[10] the micellar mole fractions (χ) and β values were calculated for the solutions examined (Table 1).

The magnitude of β is proportional to the sum of the interactions between both like and unlike surfactants in the micelle and so is coupled directly with the CMC of the two surfactants being used.[10] It is likely, therefore, that the magnitude of the β values reported here, which are larger than those reported in the related literature systems, is due to strong interactions between CTAB and $C_{16}E_8$ molecules as well as adjacent $C_{16}E_8$ molecules.

TABLE 1. Critical Micelle Concentrations (CMC), Micellar CTAB Mole Fractions (χ_{CTAB}), and Rubingh Interaction Parameter (β) Values for the CTAB/$C_{16}E_8$ Mixed System at Various Solution CTAB Mole Fractions (α_{CTAB})

α_{CTAB}	CMC (mM)	χ_{CTAB}	b	α_{CTAB}	CMC (mM)	χ_{CTAB}	b
0	7.6×10^{-4}			0.6	1.2×10^{-2}	0.181	−8.0
0.2	8.8×10^{-4}	0.059	−6.4	0.8	1.7×10^{-2}	0.244	−8.8
0.4	1.0×10^{-2}	0.122	−7.2	1.0	8.5×10^{-1}		

Both increasing and decreasing β values with increasing CTAB mole fraction have been reported in the literature. For CTAB/C_XE_Y systems with increasing β values this has been attributed to the increase in the average distance between CTAB molecules, which decreases the repulsion between CTAB molecules[4] and allows for a greater degree of bromide dissociation from the micelles.[3] Where β decreases with increasing α_{CTAB},[14] these positive changes must be canceled out by a larger negative change in β; in the case of the CTAB/$C_{16}E_8$ system, this negative influence is most likely an increase in the number of attractive CTAB−$C_{16}E_8$ interactions in the micelle as χ_{CTAB} approaches 0.5.

Two of the related literature studies also examined the variation of micellar mole fraction with total surfactant concentration beyond the CMC.[3,14] These found that, as the total surfactant concentration was increased, the surfactant molar ratio of the micelle approaches that of the solution, such that the solution and micellar mole fractions are approximately equal at a total surfactant concentration of 0.01 M. As this value is significantly below the working surfactant concentration used here, it was assumed that the micellar and solution molar ratios of CTAB and $C_{16}E_8$ were equal in the film-forming solutions.

Neutron Reflectometry. The addition of $C_{16}E_8$ to the CTAB/PEI systems results in a number of changes to the neutron reflectometry profiles (Figure 2).

For the three PEI concentrations examined there is a general decrease in the level of structure of the films with increasing $C_{16}E_8$ content, indicating a decrease in the crystallinity and/or thickness of the films relative to the 100% CTAB/PEI films. More specifically, for the concentration 1 and 1/4 films, it can be seen that there is a shift in the peak position to lower Q_Z as the percentage of $C_{16}E_8$ is increased, which can be equated to an expansion of the crystal lattice (increase in the distance between the micelle centers). In the pure CTAB/concentration 1 PEI film we previously observed that two peaks—corresponding to two distinct structures—were seen in the reflectometry profile.[2] As there is little disruption of the general shape of these joined peaks upon addition of $C_{16}E_8$ it is likely that both crystalline structures are still present. This is supported by the BAM measurements (see below). Conversely, for the concentration 1/16 PEI films the position of the strong diffraction peak in the 80% CTAB film is (within experimental error) unchanged relative to the peak in the 100% CTAB film. The shape of the peak is also of interest. Time scans on this peak (Figure 3) show that initially the peak was quite intense, but over time this intensity decreased and the peak became thinner. This shortening and thinning of the peak indicates that the crystalline regions of the film are becoming less numerous but not less organized with time. Furthermore, concurrent with the disappearance of this peak is a change in the overall shape of the reflectometry profile that suggests that there is a second type of structure forming at the surface.

This structure was partially characterized by removing the data points directly associated with the peak and then modeling the remaining points with the Parratt program (Figure 4, 1/16 PEI:80% CTAB). This characterization may be somewhat inaccurate, due to the removal of the peak from this data set; however, the fitted structure corresponds well with those of the other films modeled in Figure 4, where no peaks were observed (and thus no peak removed). Though the low level of structure

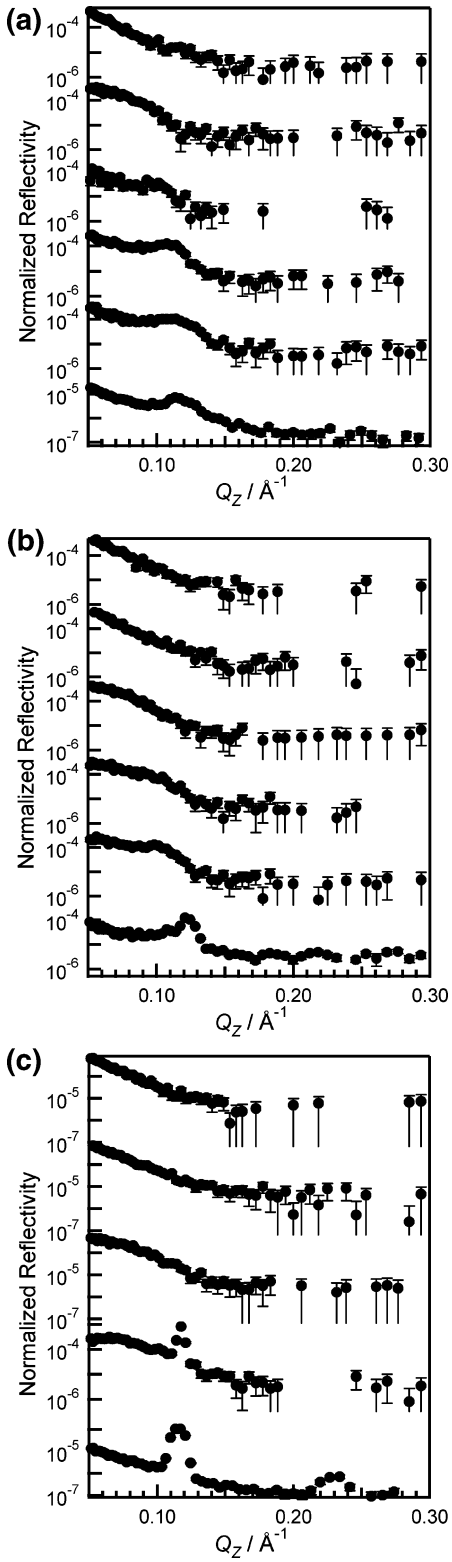

Figure 2. (a) Neutron reflectometry profiles of CTAB/$C_{16}E_8$/concentration 1 PEI films. Bottom-to-top*:* 100% CTAB, 80% CTAB, 60% CTAB, 40% CTAB, 20% CTAB, and 100% $C_{16}E_8$. (b) Neutron reflectometry profiles of CTAB/$C_{16}E_8$/concentration 1/4 PEI films. Bottom-to-top*:* 100% CTAB; 80% CTAB, 60% CTAB, 40% CTAB, 20% CTAB, and 100% $C_{16}E_8$. (c) Neutron reflectometry profiles of CTAB/$C_{16}E_8$/concentration 1/16 PEI films. Bottom-to-top*:* 100% CTAB, 80% CTAB, 60% CTAB, 40% CTAB, and 20% CTAB.

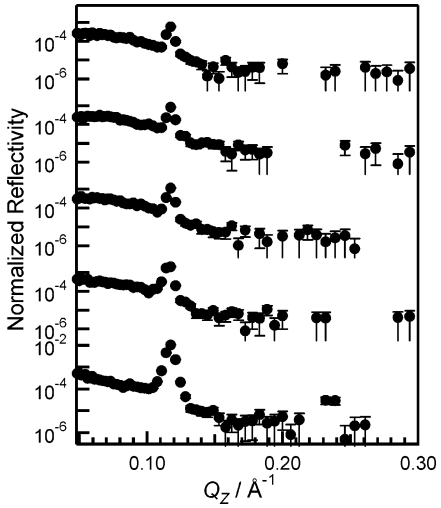

Figure 3. Time variations in the reflectometry profiles of an 80% CTAB/$C_{16}E_8$/concentration 1/16 PEI film. The reflectometry profiles correspond to (bottom-to-top) 0−15 min, 15−30 min, 30−45 min, 45−60 min, and 60−75 min.

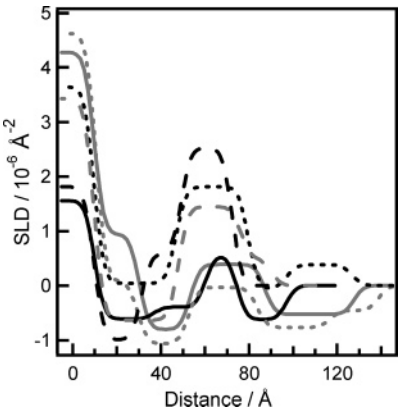

Figure 4. SLD profiles for the modeled reflectometry profiles for PEI concentration 1, 40% CTAB (solid black), 20% CTAB (solid gray); for PEI concentration 1/4, 60% CTAB (short dash black), 40% CTAB (short dash gray); and for PEI concentration 1/16, 80% CTAB (data modified, see text) (long dash black), 60% CTAB (long dash gray).

present was difficult to model well, the scattering length density (SLD) profile obtained suggests that this structure corresponds to a single ordered layer of micelles lying close to the surface with a disordered film beneath. Two scenarios are therefore possible, either the crystallites responsible for the peak are moving into solution and being replaced by less-ordered film or the crystallites are disassembling at the surface (this process would need to occur singly to each crystallite and over a fairly short period of time to give rise to the peak shape observed). If the first scenario is correct, the crystallites either break up upon removal into the subphase or remain small and widely dispersed, as no precipitates were observed in solution.

Single micelle layer models were also fitted to a number of other films where no diffraction peak was observed (Figure 4). These correspond to the 20% and 40% CTAB films at PEI concentration 1, the 40% and 60% CTAB films at PEI concentration 1/4, and the 60% CTAB film for the PEI concentration 1/16 films. An interesting feature of these profiles is the SLD determined for the subphase, which on these plots corresponds to the parts of the profile below distance = 0. Although not modeled explicitly, the SLD of the subphase gives an indication of the thickness of the films. For thinner films or ones where there is significant penetration of the solution into the film the SLD will be higher because of the presence of D_2O.

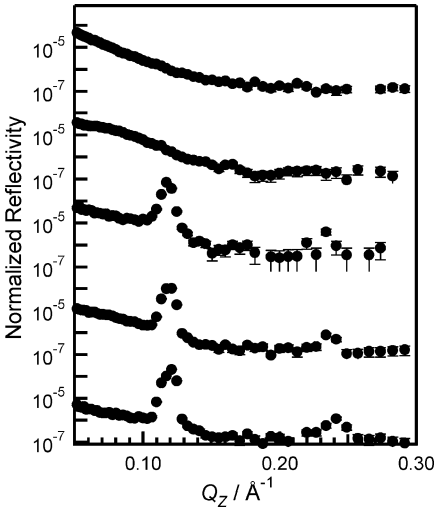

Figure 5. Neutron reflectometry profiles of CTAB/Brij56/concentration 1/8 PEI films. Bottom-to-top: 100% CTAB, 95% CTAB, 85% CTAB, 75% CTAB, and 25% CTAB.

Consequently, for all the modeled profiles it is possible to state that the films become thinner/less contiguous as the percentage of $C_{16}E_8$ increases. This is supported by the inability to model any significant structure in films with lower CTAB concentrations than the ones shown in Figure 4. Ultimately, no film was present when only $C_{16}E_8$ was used as the surfactant. The ability/inability to model the reflectometry profiles also shows that there is a decrease in the thickness and order of the films as the concentration of PEI is decreased. Interestingly, given the small mole fraction of CTAB, the presence of layers at the interface in the neutron reflectometry profile of the 20% CTAB/concentration 1 PEI film indicates that only a relatively small number of PEI−CTAB dipole−charge interactions are required to form a film.

The reflectometry profiles collected for the CTAB/Brij56/concentration 1/8 PEI system are qualitatively similar to those for the CTAB/$C_{16}E_8$ system (Figure 5). When compared with the CTAB/$C_{16}E_8$/concentration 1/16 PEI films the behavior of the two is very similar; no diffraction peak is present when the concentration of nonionic surfactant is greater than 20% and no structure is present at greater than 80% nonionic surfactant. Although this was the only experiment performed on the CTAB/Brij56/PEI system, it is unlikely that it differs greatly from the CTAB/$C_{16}E_8$/PEI system.

BAM Images. Images of the mixed films generally support the conclusions drawn from the neutron reflectometry (Figure 6). Regardless of the concentration of PEI, solutions prepared with $C_{16}E_8$ as the only surfactant failed to show any evidence of a polymer film at the air/water interface. As stated earlier, this absence of a film or any visible precipitate in the bulk indicates that there is very little interaction between PEI and $C_{16}E_8$ at the pH where the experiments were carried out.

At PEI concentration 1 all the mixed films exhibited the double fractal structure previously observed in the 100% CTAB films, which gives rise to the two peaks in the neutron reflectometry profiles.[2] Surprisingly, as the percentage of $C_{16}E_8$ increases, the BAM images show a movement away from and then back to the manner of film growth exhibited by the 100% CTAB film. In the 60% CTAB film the fractal structures grow in a more compact manner and the two structures are only visible late in the film growth, whereas the 20% CTAB film grows in a fashion similar to the 100% CTAB film. As there are no significant changes in the reflectometry profiles of any of the concentration 1 films with time and the trends in the profiles

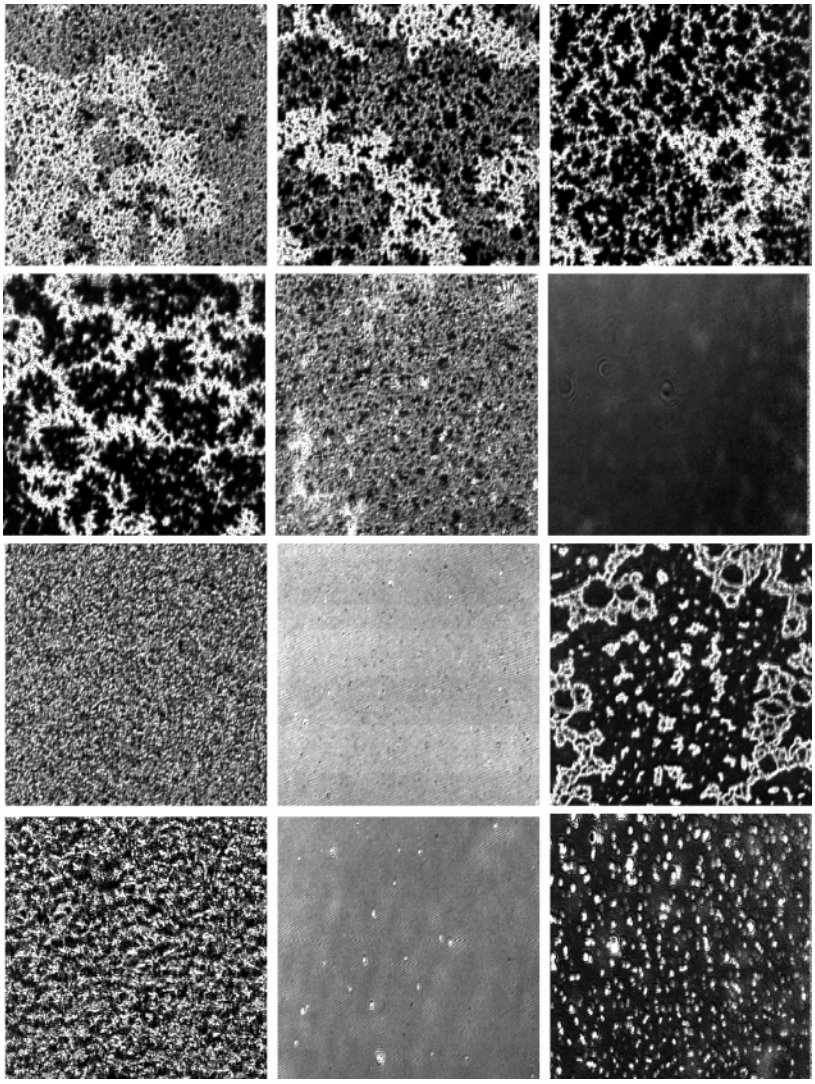

Figure 6. BAM images of CTAB/$C_{16}E_8$/PEI films with polymer concentrations and CTAB mole percentages of (top row) PEI concentration 1 with 100, 80, and 60% CTAB; (second row) PEI concentration 1 with 40, 20, and 0% CTAB; (third row) PEI concentration 1/4 with 100, 60, and 20% CTAB; (bottom row) PEI concentration 1/16 with 100, 60, and 20% CTAB. The images were taken 30 min after mixing and are 300 μm $\times$ 300 μm in size.

brought about by the addition of $C_{16}E_8$ are constant, this variation in macroscopic growth behavior of the films must have little effect on the mesoscopic organization of the films.

For both the PEI concentration 1/4 and 1/16 systems the images show a general decrease in the contiguity of the films with increasing $C_{16}E_8$. For the 1/16 films the BAM images for the 100% CTAB and 80% CTAB films are very similar, with both showing an apparently rough but distinct film; however, for the remaining films the film appears to become smooth and speckled. These changes correspond relatively well with the neutron reflectometry results, so it is likely that the loss of mesostructure from the film and the change in the morphology of the surface are related.

The BAM images reported here differ slightly from those reported in a previous paper,[2] with the structures in the PEI concentration 1 and 1/4 films forming larger domains here. This is most likely due to the change in evaporation conditions experienced by the films (an important factor in the formation of these film), as the poly(tetrafluoroethylene) troughs used here have a larger surface area-to-volume ratio than the polystyrene dishes used previously.

SANS. SANS data were collected on 70% mole ratio CTAB/$C_{16}E_8$ solutions with PEI concentrations of 1, 1/2, 1/4, and 1/8 and on 50% mole ratio CTAB/$C_{16}E_8$ solutions with PEI concentrations of 1 and 1/2. A sample, showing the measured data and fit, is given in Figure 7 and the calculated parameters are given in Tables 2 and 3 and Figure 8. For reasons outlined in the Experimental Section, all the systems were fitted to a prolate (rugby ball-shaped) ellipsoid model.

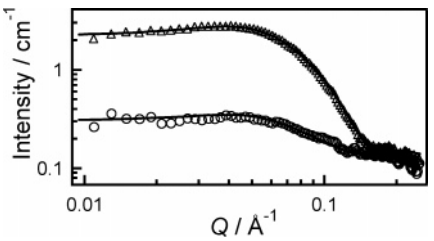

Figure 7. SANS profiles for the two contrasts used for the 70% CTAB/concentration 1 PEI system with their modeled fits: CTAB with 100% D_2O (triangles) and D33-CTAB with 40% D_2O (circles).

In general terms, there is little change in the shape of the micelles in the presence of PEI, although there may be a slight trend toward more spherical micelles with decreasing polymer concentration, which is consistent with the results from CTAB with PEI,[2] though the change is distinctly smaller in the CTAB/$C_{16}E_8$ micelles (Figure 8). Prolate micelles are also formed for

TABLE 2. SANS Model Parameters for the CTAB/$C_{16}E_8$/PEI Solutions[a]

	70%CTAB				50% CTAB	
PEI concn	1	1/2	1/4	1/8	1	1/2
R(a)/Å	34	33	35	32	36	38
R(b)/Å	24	25	25	26	24	25
SLD $1/10^{-6}$ Å^{-2}	6.02	6.43	6.16	6.42	5.69	5.46
SLD $2/10^{-6}$ Å^{-2}	1.82	2.15	2.70	3.44	2.28	2.28
salt concn/M	0.033	0.017	0.010	0.006	0.028	0.015
vol fraction	0.0119	0.0115	0.0129	0.0119	0.0134	0.0167

[a] SLD 1 and 2 refer to the SLD difference between the micelle interior and the surrounding solution for the CTAB/$C_{16}E_8$/D_2O and D33-CTAB/$C_{16}E_8$/40% D_2O systems, respectively. The errors associated with the SLD values are $\pm 5 \times 10^{-8}$, while for salt concentration, volume fraction, and radii values the errors were $\leq$10%, $\leq$5%, and approximately 1 Å, respectively.

TABLE 3. SANS Model Parameters for the CTAB/$C_{16}E_8$ Solutions[a]

CTAB	70%	50%
R(a)/Å	38	38
R(b)/Å	25	26
SLD $1/10^{-6}$ Å^{-2}	6.42	6.69
SLD $2/10^{-6}$ Å^{-2}	3.68	3.79
salt concn/M	0.00	0.00
vol fraction	0.0157	0.0157

[a] SLD 1 and 2 refer to the SLD difference between the micelle interior and the surrounding solution of the micelles in 100% D_2O and 60% D_2O, respectively. The errors associated with the SLD and the salt concentration values are $\pm 5 \times 10^{-8}$ and $\leq$5%, respectively, while for the volume fraction and radii values the errors were $\leq$3% and approximately 1 Å.

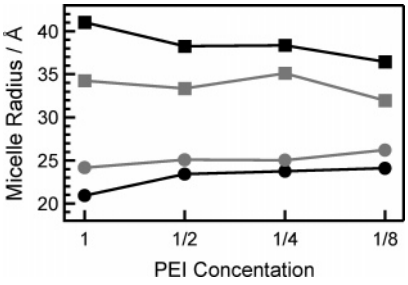

Figure 8. The major [*R*(a), squares] and minor [*R*(b), circles] radii for the micelles of the CTAB/PEI[2] and 70% CTAB/PEI systems (black and gray lines, respectively) as a function of the polymer concentration.

CTAB and $C_{16}E_8$ without PEI. These appear to be larger than the micelles formed in the presence of PEI; however, this may be due to values of the other variables used in the model. For both the 70% and 50% CTAB systems without PEI, the volume fraction of the micelles in solution is significantly larger than the volume fraction calculated for the surfactant alkane chains (0.0114). Therefore, the ellipse defined by these models is likely to include not only the hydrocarbon core of the micelles but also some of the headgroup region as well. This is supported by the lower than expected SLD contrast (the difference between the SLDs of the micelle/ellipse interior and the solution) of the micelles. As the SLD of the surfactant headgroups is relatively high compared to the alkane chains (i.e. closer to D_2O), the SLD contrast calculated by the model will be lower, if headgroups are incorporated, than would be calculated if the model defined the ellipse as the alkane core alone. There are insufficient contrasts available to allow fitting of a more complex model, such as a core−shell ellipse, which could better represent the true micelle structure.

The same interpretation may also be applied to the 50% CTAB/PEI systems, which both have higher volume fractions and variant SLD contrasts. Conversely, for the 70% CTAB/PEI systems (excluding PEI concentration 1/4), the calculated volume fractions are fairly close to those for the alkane core alone and the SLD contrasts are reasonably close to those calculated for surfactant micelles in a homogeneous solution of polymer. The micelle aggregation numbers of these three 70% CTAB/PEI models with volume fractions close to the theoretical volume fraction were determined to be 165, 173, and 180 for the micelles with concentrations 1, 1/2, and 1/8 PEI, respectively. Therefore, with increasing PEI concentration it would appear that there is a decrease in the micelle aggregation number.

It should be noted that a direct comparison of the theoretical and modeled SLD contrasts could not be done with certainty as variations in the micelle sizes with polymer concentration clearly indicate that the polymer is interacting with the micelles, and therefore, the polymer solution cannot be homogeneous. Again, ideally, a more complex model, such as a core−shell ellipsoid model, should be used; however, the data obtained is insufficiently detailed to allow for resolution of more parameters. (This could rectified by performing more SANS experiments with different contrasts; however, due to neutron experiment time constraints, we were not able to perform these experiments.)

A comparison of the radii of the micelles in the 70% CTAB/PEI solutions with the equivalent pure CTAB/PEI[2] solutions shows that the micelles formed by pure CTAB in the presence of PEI are more elongated than those of the mixed surfactants; however, the volumes of the micelles and their variations with PEI concentration are very similar (Figure 8).

The similar micelle volumes for all CTAB/$C_{16}E_8$ compositions observed here contrast with work reported in the literature on mixed CTAB/Brij56 micelles that showed an increase in the aggregation number (and therefore size of the alkane core) of the micelles with increasing percentages of nonionic surfactant.[9] However, as no SANS measurements were performed on the CTAB/Brij56 system, no direct comparison with this work is possible. The literature also reports SANS experiments on CTAB/$C_{16}E_6$[15] and dihexadecyldimethylammonium bromide (DHDAB)/$C_{12}E_6$ systems.[16] For the CTAB/$C_{16}E_6$ system, a strong interaction is reported at relatively low ($\geq$10%) CTAB mole percentages, and the addition of CTAB tends to increase the curvature of the micelle surface compared with pure $C_{16}E_6$. Again, this would appear to be contrary to the results reported here. The second system of DHDAB/$C_{12}E_6$ is more removed from the system reported here in that the cationic surfactant has two alkyl chains, while the nonionic surfactant has a far shorter alkane chain. For this system, although elliptical micelles are formed, the shape and aggregation number of these micelles is not linear with the micelle composition (between 10 and 50% DHDAB). Generally, the aggregation numbers reported for these micelles were smaller than the aggregation numbers reported here; at 50% DHDAB the aggregation number was 156. For the solutions without PEI, when the radii modeled here are compared with those of CTAB micelles (including the headgroups) reported elsewhere [*R*(a) $\approx$ 43.1 Å and *R*(b) $\approx$ 28.7 Å at 0.12 M CTAB],[17] it appears that the surfactant micelles become more elongated with increasing CTAB mole percentage, as is the case for the solutions with PEI.

From the neutron reflectometry and BAM experiments, it is apparent that as the amount of nonionic surfactant in the micelles increases there is a loss of interaction between the surfactant micelles and the polymer at the air/water interface. The SANS measurements are inconclusive as to whether this is mirrored in the bulk, though we would expect this to be the case.

If there were a loss of interaction it would probably be due to an absence of interaction between the polymer and the nonionic surfactant. To the best of our knowledge, no significant PEI−alkyl poly(ethylene glycol) interaction has been reported in the literature; thus, any electrostatic interaction between these two is relatively weak or absent and the incorporation of $C_{16}E_8$ into the micelle will not assist in polymer association with the micelles. The effect of this noninteraction could be magnified by the difference in the size of the headgroups of the cationic and nonionic surfactants. The nonionic surfactants have linear hydrophilic headgroups that are believed to extend into the bulk solution and are significantly solvated, while CTAB has a bulky yet compact headgroup. Consequently, a high mole fraction of the nonionic surfactant could physically shield the cationic surfactant from the polymer in solution.

Conclusions

Surface tension, SANS, BAM, and neutron reflectometry were used to characterize the effect that addition of the nonionic surfactants $C_{16}E_8$ and Brij56 had on the formation of CTAB-templated PEI films. Generally, the nonionic surfactants decreased the thickness of and degree of ordering in the films; however, for the 20% CTAB/80% $C_{16}E_8$/concentration 1 PEI solution, a surface film with some structure was still observed, despite the low CTAB concentration. This suggests that the number of PEI−CTAB dipole−charge interactions needed to form films at the air/water interface is fairly small. The surface tension and SANS measurements indicated that there is a strong interaction between CTAB and $C_{16}E_8$, in solution micelles, although these micelles do not interact strongly with the polymer in the subphase solution. The similarity between the neutron reflectometry profiles of CTAB/$C_{16}E_8$/concentration 1/16 PEI and CTAB/Brij56/concentration 1/8 PEI suggests that the behavior of these two systems is similar.

Acknowledgment. We thank Dr S. Holt and Dr S.M. King for assistance with the neutron experiments on SURF and LOQ, ISIS. This work has been financed by the EPSRC (GR/S84712/01) within the EUROCORES Program SONS of the European Science Foundation, which is also supported by the European Commission, Sixth Framework Program. K.J.E. thanks the Royal Society for a Dorothy Hodgkin Research Fellowship.

References and Notes

(1) Edler, K. J.; Goldar, A.; Brennan, T.; Roser, S. J. *Chem. Commun.* **2003**, 1724−1725.
(2) O'Driscoll, B. M. D.; Milsom, E.; Fernandez-Martin, C.; White, L.; Roser, S. J.; Edler, K. J. *Macromolecules* **2005**, *38*, 8785−8794.
(3) Rodenas, E.; Valiente, M.; del Sol Villafruela, M. *J. Phys. Chem. B* **1999**, *103*, 4549−4554.
(4) Carnero Ruiz, C.; Aguiar, J. *Colloids Surf. A.; Physiochem. Eng. Aspects* **2003**, *224*, 221−230.
(5) Penfold, J.; Staples, E.; Tucker, I. *Adv. Colloid Inter. Sci.* **1996**, *68*, 31−55.
(6) Penfold, J.; Staples, E. J.; Tucker, I.; Thomas, R. K. *Colloids Surf. A.; Physiochem. Eng. Aspects* **1999**, *155*, 11−26.
(7) Gao, H. C.; Zhu, R. X.; Yang, X. Y.; Mao, S. Z.; Zhao, S.; Yu, J. Y.; Du, Y. R. *J. Colloid Interface Sci.* **2004**, *273*, 626−631.
(8) Zakharova, L.; Valeeva, F.; Zakharov, A.; Ibragimova, A.; Kudryavtseva, L.; Harlampidi, H. *J. Colloid Interface Sci.* **2003**, *263*, 597−605.
(9) Chakraborty, T.; Ghosh, S.; Moulik, S. P. *J. Phys. Chem. B* **2005**, *109*, 14813−14823.
(10) Rubingh, D. N. Mixed Micelle Solutions. In *Solution Chemistry of Surfactants*, Mittal, K. L., Plenum: New York, 1979; Vol. 1, pp 337−353.
(11) Clint, J. *J. Chem. Soc., Faraday Trans. 1* **1975**, *17*, 1327−1334.
(12) Parratt, L. G. *Phys. Rev.* **1954**, *95*, 359−369.
(13) Hayter, J. B.; Penfold, J. *Mol. Phys.* **1981**, *42*, 109−118.
(14) Guo, W.; Sun, Y. W.; Luo, G. S.; Wang, Y. J. *Colloids Surf. A.; Physiochem. Eng. Aspects* **2005**, *252*, 71−77.
(15) Cummins, P. G.; Penfold, J.; Staples, E. *Langmuir* **1992**, *8*, 31−35.
(16) Penfold, J.; Staples, E.; Tucker, I.; Thomas, R. K. *Langmuir* **2004**, *20*, 1269−1283.
(17) Berr, S. S.; Caponetti, E.; Johnson, J. S.; Jones, R. R. M.; Magid, L. J. *J. Phys. Chem.* **1986**, *90*, 5766−5770.